

Phoenix (PHX) Project

MET Pressure & Temperature

Characterization & Calibration Report



Version 1.0

Prepared by:

Peter A Taylor, Di Wu , Stephen Brown, Konstantin Baibakov,
Carlos F. Lange and Jeff Davis

MET Document Manager:

Cameron Dickinson

<p>Prepared by:</p> <hr/> <p>Cameron Dickinson Phoenix MET Team</p>	<hr/>
<p>Approved by:</p> <hr/> <p>Jim Whiteway Instrument Co-Investigator, MET</p>	<hr/> <p>Leslie Tamppari Phoenix Project Scientist</p>
<hr/> <p>Dr. Reta Beebe Director, PDS Atmospheres Node</p>	<hr/> <p>Ed Grayzeck Project Manager, Planetary Data System</p>

Revision and History Page

Rev.	Description	Date
1.0	Document Start	03/03/08

TBD Items

Section	Description

1	Purpose and Scope of Document.....	5
2	Applicable Documents.....	5
3	Introduction.....	5
4	CSIL MARS WIND TUNNEL FACILITY.....	7
4.1	SWITCHED FLOW TEST SECTION AND PROCEDURES.....	9
4.2	SOLAR RADIATION TEST SECTION AND PROCEDURES.....	9
4.3	WIND TUNNEL RESULTS – TIME CONSTANT FROM FLOW SWITCHING	11
4.4	WIND TUNNEL RESULTS – TIME CONSTANTS AND TEMPERATURE INCREASES FROM SOLAR RADIATION IMPACTS.....	12
4.5	DUST IMPACTS.....	14
4.6	LAMINAR FLOW IN A RECTANGULAR DUCT.....	14
4.7	NUMERICAL FLOW AND HEAT TRANSFER MODELLING.....	15
5	CONCLUSIONS.....	16
6	ACKNOWLEDGEMENTS.....	17
7	REFERENCES.....	17
	Appendix A. List of Tables.....	19
	Appendix B. List of figures.....	21

1 PURPOSE AND SCOPE OF DOCUMENT

This document provides users of the Phoenix MET (Meteorological) data products with a detailed description of the characterization activities relating to the Pressure and Temperature sensors.

It is intended to provide enough information to enable users to read and understand background information relating to the data products. The users for whom this document is intended are the scientists who will analyze the data, including those associated with the project and those in the general planetary science community.

The Phoenix Mars lander is equipped with a 1m mast. At three levels on the mast C-frames are mounted, each holding three fine-wire, fast-response, thermocouple sensors to measure air temperatures. There is no radiation shielding and we need to know the time constant of these units and their response to solar radiation, both in a Mars environment and as they vary with wind speed. In order to achieve this a small Mars wind tunnel facility was constructed and used to characterize identical thermocouple units to those on the Phoenix lander. The facility is described together with results of the thermocouple characterization tests and some numerical studies designed to explain the temperature distribution within the wind tunnel test section.

2 APPLICABLE DOCUMENTS

[1] MET PT SIS Document

[2] MET PT EDR/RDR Archive Volume SIS Document

3 INTRODUCTION

Air temperatures will be measured at three heights (0.25, 0.5 and 1.0m) on a mast above the deck of the Phoenix Mars lander. They will be measured with standard fine wire, 75 μm diameter, butt welded Chromel-Constantan thermocouples coupled with a resistance thermometer in an isothermal block housing the “cold” junctions of the thermocouples. As described in Taylor et al (2008) the Flight Model units at each level have three thermocouples in parallel in a small C frame and each unit has been calibrated in isothermal baths (see Taylor et al, 2007). For the tests described here identical thermocouples have been used with very similar or identical C frames. The primary focus is on determining the time constant of the thermocouples and determining the potential impact of solar radiation on the “hot” junctions. Both of these effects will vary with wind speed past the thermocouples and testing to simulate this in a Mars environment was a mission requirement. Very similar 0.75 μm diameter thermocouples were used on the Viking landers (see Chamberlain et al, 1976) while those on Pathfinder (Seiff et al, 1997) were constructed differently and had a longer time constant.

Tillman et al (1994), extrapolating from a report by Davey et al indicate a “worst case” time constant for the Viking thermocouples as in a range “from 1.3 to 0.98 s or less” and they used a time constant of 1.0 s in their analyses appropriate to the Viking lander sites, where pressures ranged from about 7 to 10 hPa. For the Pathfinder thermocouples Schofield et al (1997) give the time constant as “1 to 2 seconds”. For the Phoenix thermocouples we sought to determine the time constants experimentally in a Mars environment.

To achieve this, a small wind tunnel unit was designed and constructed in the Centre for Research in Earth and Space Science (CRESS) Space Instrumentation Laboratory (CSIL). This could be installed inside a 1m diameter vacuum chamber which was then evacuated and backfilled with carbon dioxide to pressures of 6-8 hPa to represent the Mars atmosphere. The whole unit could be cooled to Mars temperatures (typically -20C to -70C). The wind tunnel unit was in fact a dual tunnel arrangement with very rapid switching of airflow from one stream to another through the test section. One stream was heated to several degrees warmer than the other and switching from one stream to the other was used for time constant determination.

The goals of the investigation of the performance of the thermocouple systems were:

- 1) Accuracy: To test the performance of the thermocouples in a Mars environment.
- 2) To determine the time constant of the thermocouples in the Mars atmosphere over a range of wind speeds.
- 3) To test the effect of simulated solar radiation on the thermocouples in the Mars atmosphere over a range of wind speeds.

Determination of the time constant, and its dependence on wind speed is important to ensure that the sensors accurately report any sudden changes in temperature which might be expected in micro-fronts, dust-devil passages or other features. A short time constant is also necessary to ensure accurate determination of temperature standard deviation and skewness. These statistics of the temperature data may be used, in conjunction with Monin-Obukhov similarity theory to infer heat and momentum fluxes at the surface and to provide estimates of wind speed at times when other Phoenix sensor information (from the telltale or TECP needle – see Gunnlaugsson et al, 2008 and Zent et al, 2008) are not available.

Three methods of causing a sudden temperature change in the gas flow were considered. The first was to put a heating element or grid immediately in front of the thermocouple. Although this would have given almost instantaneous heating of the gas, the cooling would have been dependent on the speed at which the gas cooled the heater. The second was to heat the thermocouples by putting a current through them, and then measure the time constant of the temperature drop after the current was turned off. The third method, which was adopted, was to switch the thermocouples quickly between two gas streams of different temperatures. Although mechanically more complicated, the switching approach had the advantage of producing time constants for both rising and falling temperatures. Corroborative data on the time constant will also be obtained from solar radiation impact tests, and indeed these allowed us to extend the time constant values to lower wind speeds than we have used with switched flow technique.

The thermocouples are not shielded from solar radiation and will be heated by the sun. Given the low density of the Mars atmosphere, conduction of heat to the air from the thermocouples

will be less effective than on Earth and an accurate assessment of the impact of solar radiation on the thermocouples in conditions appropriate to Mars is essential.

It is perhaps worth adding that it proved impossible to detect the location of the thermocouple junction by visual inspection, even with the aid of magnifying eyepieces. The manufacturer indicates the junction location on the cards on which the thermocouples were mounted but these may not have been checked and there is also a potential for error in the process of mounting the thermocouples in the C-frames. It is thus necessary to check the location of the junction. This can be done by illuminating the wire with a narrow but intense light beam while monitoring the temperature reported. The temperature shows a marked increase when the beam is shone directly on the Chromel-Constantan junction and in this way the location can be checked to within about 1 mm. One of the units supplied to us was found to have one wire with the junction completely out of the opening while in another case we found that one of the three thermocouples had its Chromel and constantan wires reversed. Additional quality assurance checks have been implemented.

4 CSIL MARS WIND TUNNEL FACILITY

Before proceeding with the development of the CSIL Mars wind tunnel facility we considered other options for conducting the experiments. Among them were to use the Oxford University Low Density Wind Tunnel Facility (LDWT), the Mars Wind Tunnel at Aarhus University, Denmark and the NASA Mars surface wind tunnel facility at Ames.

The Oxford University Low Density Wind Tunnel was adapted and used for testing and calibration of the Beagle 2 wind sensor (see <http://www.atm.ox.ac.uk/user/wilson/matacf.html>). It is an open circuit wind tunnel, with CO₂ being drawn from a large reservoir into a low pressure test section and then vented. All testing to the date of our studies had however been conducted at ambient temperature and to add a cooling system would have made the use of this facility too costly.

The Mars simulation wind tunnel at Aarhus University is a re-circulating wind tunnel (see, <http://www.marslab.dk/WindTunnel.htm>) that is enclosed inside a vacuum chamber. This chamber can be filled with gas (CO₂) and brought down to Mars-like pressures of 5-10mbar. Small dust particles of a Mars analogue soil are injected into the wind stream to further simulate Martian atmosphere. These particles also provide a means for measuring wind speeds with a laser Doppler Anemometer. The Aarhus tunnel is being used for testing of the Phoenix telltale wind sensor but was not considered ideal for our purposes.

At the Ames Research Centre, NASA operates a Mars surface wind tunnel facility within a large vacuum chamber. It concentrates on aeolian processes and has a large test section but was not considered appropriate for our tests.

Table 1 lists the essential characteristics of the Oxford and Aarhus wind tunnels as well those of the CSIL Mars Wind Tunnel.

Based on the costs and limitations of other facilities, we were persuaded that the best approach was to build our own small wind tunnel to fit inside a vacuum chamber that was available at CSIL. This also gave us time to test and develop a novel flow switching feature to determine time constants, and to set up a suitable solar radiation test procedure. As a result a small Mars wind tunnel was built at York University to determine the response of the PHOENIX thermocouples to sudden changes in atmospheric temperature and to determine the effect of solar radiation on unshielded thermocouples. The tests were conducted at typical Mars temperatures and pressures but the same facility and procedures could be applied to other conditions, for example those applicable to Earth's upper atmosphere. Since we developed the wind tunnel facility CSIL have acquired a much larger thermal controlled vacuum chamber and the wind tunnel unit could easily be used in that, or a larger scale tunnel could be built to the same design.

The CSIL dual wind tunnel (Figs 1, 2) was designed to fit within an existing CSIL pressure chamber (Fig 2). This limited the tunnel size to 1.2 metres length and 1 metre diameter. Because the chamber did not have its own cooling system, a cooling channel was built into the tunnel. To insulate the tunnel from the room-temperature chamber walls, aluminium-clad foam tape was applied to the tunnel exterior. Once the test thermocouples were installed, an envelope of metallized plastic was fitted over the entire assembly to enclose a volume of cold gas around the tunnel. A second metallized layer was then added for extra insulation.

Once installed in the chamber the pressure is reduced to near vacuum (0.53 hPa) and the whole wind tunnel unit is cooled by pumping LN2 through cooling pipes within it. The cooling Set Point for the wind tunnel testing was initially -70C. Once that is reached we input CO2 at the desired pressure, generally 8 hPa. One tunnel has a heating strip attached to warm the air (CO2) in that tunnel by up to 5K above that in the other tunnel.

Two mirror-image tunnels were built, separated by a 3 cm insulating gap to allow them to operate at slightly different temperatures. Two fans, mounted on a common shaft, were driven by a single adjustable-speed motor. Each wind tunnel half (warm and cold) has a 64 mm long, wide-angle diffusion section that expands the cross section from the size of the fan outlet (113 mm x 55 mm) to the size of the settling section (150 mm x 145 mm). The settling sections are 60 mm long and filled with plastic tubes (drinking straws) 6 mm diameter that serve as the "honeycomb". There are two screens, one immediately in front of the honeycomb and one immediately following. The screens are made of 0.25 mm diameter wire on a 1.5 mm spacing. The contraction sections that follow are 174 mm long. These two sections merge in front of the switching blades which continue the reduction in cross section to that of the single test section, 25 mm x 25 mm, slightly larger than the opening in the thermocouple frame. The test section in this configuration is 100 mm long. The flow then splits again into two, 200 mm-long, narrow-angle diffusers that expand at 10 degrees x 5 degrees. The expansion continues around a 70 mm radius bend to reverse the flow direction back towards the front of the chamber. The expansion continues for another 500 mm, and is then channelled into two circular, flexible ducts and back to the fans.

The test sections of the tunnel are removable. Two sections were built: one to use for measurements of the time constants of the thermocouples with switching between gas flows of different temperatures and one for measurements of the effects of solar radiation. Both tests are

to be conducted at a variety of wind speeds. The Chromel and Constantan wires that are part of the thermocouple assemblies are long enough to reach an isothermal block inside the chamber directly. The isothermal block is thermally connected (bolted with lots of area and thermal compound) to the chamber wall, the outside of which remains at room temperature throughout the test. Because the block, the vacuum connectors and the data logger are all at the same temperature, the connections from the isothermal block to the connector and to the data logger were made using ordinary, tin-coated copper hook-up wire.

4.1 SWITCHED FLOW TEST SECTION AND PROCEDURES

A photograph of the flow-switching test section is shown in Figure 3. Switching was performed using four vanes driven by a single permanent-magnet actuator. The vanes were switched once every fifteen seconds from the beginning of the cool-down period until the end of the test. The temperature difference between the two tunnels was created by a heater strip attached to the test section on one tunnel only. The temperature difference was typically 3C.

Wind speed was measured using a Dwyer 3 mm diameter Pitot tube (Fig 3) located just downstream of the thermocouples under test and connected to an externally mounted MKS 223BD differential capacitance manometer with an analogue output of 27 Pa / Volt. Because of the low pressure, the readings were usually less than 10 mV. Isolation and cross-feed valves were installed for zero readings, but the movement of the valves caused large excursions in the output. Most zero tests were conducted with the fan turned off temporarily.

The Reynolds number (Re) for the flow, based on a wind speed of 10 ms^{-1} , the channel height (25 mm) and the kinematic viscosity of CO_2 at -30 C ($7.15 \times 10^{-4} \text{ m}^2\text{s}^{-1}$) is of order 350 and below the critical Re for 2D channel or pipe flow (about 2,000). As a result and assuming a laminar flow profile, the Pitot reading only applied to the centre line of the test section. For some tests a thermocouple assembly was modified by removing two of the thermocouple wires so that only the wire with the junction aligned in front of the Pitot tube was used. Note also that, based on the thermocouple wire diameter ($75 \mu\text{m}$) and with $U = 10 \text{ ms}^{-1}$, $Re = 1.05$.

Air temperatures in the two tunnels are monitored by platinum resistance thermometers attached to small copper blocks suspended in the airstreams. In fact we have found quite strong temperature gradients throughout the wind tunnel unit despite wrapping it with thermal insulation. This has no impact on the time constant determinations but it did pose problems with establishing the accuracy of the thermocouple temperatures in a Mars environment with this set-up. Numerical modelling of heat diffusion in the laminar flow, described in a later section of this paper, explains why these gradients were present.

4.2 SOLAR RADIATION TEST SECTION AND PROCEDURES

For the solar irradiance test, both tunnels were operated at the same temperature. The two gas streams were combined in a test section lined with white-painted Styrofoam insulation. The light source was installed outside of the chamber and light was focused onto the end of an optical fibre bundle mounted just inside the pressure window. The other end of the fibre bundle aimed the light at the test thermocouple junction through a window in the base of the test

section. All of the optics were made of fused silica in order to pass ultra-violet light as well as the visible and near-infrared. The top of the test section was made of clear acrylic to allow the light to leave the test section rather than being absorbed by the walls.

Two thermocouples were installed for all irradiance tests. The thermocouple to be tested was located at the rear of the test section in the area illuminated by the xenon lamp. A reference, non-illuminated, thermocouple was located at the front of the test section.

Because of space limitations, no collimation optics were installed between the fibre bundle and the test thermocouple. As a result, the illumination of the thermocouple wires was not as uniform as might have been desired. The inside edges of the fibreglass frames were also illuminated, although most of the frame was shaded by the Styrofoam insulation, which also served as a support.

The test consisted of opening the shutter to illuminate the thermocouples, leaving them illuminated for up to twenty minutes, then closing the shutter and allowing the thermocouples to cool, for up to another twenty minutes. The initial temperature rise took place within approximately one second of the illumination. The thermocouples then continued to warm at a slower rate until the end of the illumination period, at which time the temperature drift matched that of the un-illuminated reference thermocouple.

The solar spectrum at the surface of Mars was assumed to have the same shape as the spectrum above the atmosphere. The irradiance values were taken from the American Society for Testing and Materials, ASTM E490 standard for solar radiation above Earth's atmosphere and then scaled to the orbit of Mars. Atmospheric absorption was assumed to be 30%, applied equally from 250 nm to 2000 nm. The final irradiance was 0.299 x the ASTM values.

A 150 Watt Xenon lamp supplied the illumination for the tests. The optical train included two lenses, a pressure window and a fibre bundle, all made of fused silica. One AM0 atmospheric filter was used to reduce the line emissions that occur between 750 nm and 1000 nm. Despite the use of the filter, the lamp irradiance significantly exceeds the desired irradiance in this range (as shown in Figure 4). The spectral shape of the light from the lamp /AM0 filter / fibre bundle optical train was measured from 250 nm to 2000 nm. The optical train spectrum was then scaled to match the expected solar spectrum on Mars. A reasonable fit occurred when the optical train irradiance at 650 nm was made equal to the expected solar irradiance at that wavelength. The integrated lamp spectrum from 250 nm to 2000 nm was 476 Wm^{-2} compared to the target integration of 379 Wm^{-2} . A silicon diode with a band-pass filter was calibrated to measure the surface irradiance at 650 nm. That diode was later placed in the wind tunnel at the position of the middle of the centre thermocouple while the lamp optics were adjusted for the correct intensity.

Taking the solar constant for Mars as 591 Wm^{-2} and a relatively low optical depth as 0.2 we would have irradiance at the surface of 483 Wm^{-2} normal to the sun's rays. The tests therefore correspond to the maximum likely impact of solar radiation on the thermocouples.

As noted earlier, the irradiation of the thermocouple wires was not as uniform as desired. Normalized to the irradiance at the middle of the centre thermocouple wire, the irradiance at

the middles of the top and bottom wires were 82% and 90%. Eight millimetres either side of the middle, the irradiance values decreased to 82%, 80% and 75% of the middle values for the top, centre and bottom thermocouples respectively. It was therefore decided that, in order to obtain uniform irradiation, the top and bottom wires of thermocouple unit were removed and only the middle wire was used in these tests. Measurements were made assuming that the junction of the thermocouple is at the center of the wire between the two sides of the frame.

For these tests the chamber was pumped to less than 0.5 hPa, and then liquid nitrogen was sprayed into the cooling channel to lower the tunnel temperature. Once the chamber had reached the target temperature of -70C, the cooling was turned off. To avoid solidifying the CO₂ atmosphere, the chamber was kept under vacuum until the tunnel temperature had risen above -70C. The CO₂ gas was then admitted, and measurements made while the tunnel warms.

During the tests we noted a rather surprising change in the temperature difference with and without our simulated solar radiation at temperatures below -40C as shown in Figure 5. This appears to be a result of a substantial loss of transmission by the optical fibres for $T < -40$ C and these data could not be used for irradiance effect calculations. They can however be used for estimates of the time constant when the lamp is turned off. Other possibilities were explored (CO₂ freezing, H₂O ice formation) and eliminated and we are reasonable certain that it is an optical fibre transmission problem.

To verify constancy of the lamp, we traced the side intensity every five minutes and the result showed that after one hour with the lamp on, the irradiance remained within 3% around the desired value. We kept the lamp on during our following tests, and used a piece of aluminium to block the irradiance rather than turning off the lamp.

The test procedure started by setting and taking the measurements of pressure, wind speed, and reference temperature. The pressure was set to about 6 Torr (8 hPa) for each test. We controlled the wind speed by adjusting the motor voltage, and the wind speed was then calculated from the corresponding Pitot pressure difference. After that, we recorded the reference temperature. The next step was to direct light from the lamp onto the thermocouple and record the time. The third step, up to 20 minutes later was to turn the irradiation off by blocking the light. We then waited up to another 20 minutes before taking the measurements of pressure, wind speed, reference temperature again. A series of measurements were made over a several hour period during which the chamber warmed from an initial temperature near -60 C to room temperature. Initial tests were also conducted at room temperature over a range of wind speeds.

4.3 WIND TUNNEL RESULTS – TIME CONSTANT FROM FLOW SWITCHING

The thermocouple unit tested was one constructed at York to closely approximate those being manufactured for Phoenix by MDA. It comprises three Omega fine-wire (75 µm diameter), butt-welded, type E (Constantan-Chromel) thermocouples mounted, in parallel, on a C-frame and connected with thermocouple grade Constantan and Chromel wires to an isothermal block containing a resistance thermometer (the “cold” junction). Thermocouple voltages were recorded by a Campbell CR10X data logger.

Our main test run was conducted on 18 Aug 2005. We used 6 wind speeds between 4.5 and 27.7 ms⁻¹ (see Table 2). At each wind speed, after allowing the system to settle down, we collected three minute data from the CR10X and took five temperature decreasing and increasing cycles to calculate the time constant at each wind speed. Sample data are shown in Figure 6. We attribute the small temperature jumps at the end of some of the high temperature intervals to temperature variation across the flow and some unsteadiness in the flow at the instant that it is switched. In this range of wind speeds the full temperature adjustments took up to about 1.2 s. The original temperature was determined as the average temperature during 2 seconds before the change started and the final temperature was the average temperature of 2 seconds after the change was considered to have finished.

The temperature data were plotted on a log scale (Fig 7). The slope of the line then determines the time constant. This is based on the assumption that the rate of change of temperature is proportional to the temperature difference between the wire, at temperature T_t and the surrounding air at temperature T_a , i.e. $d(T_t - T_a)/dt = -(T_t - T_a)/\tau$ where τ is the time constant so that, with $t = 0$ at the switch from one air stream to the other and assuming that T_a is approximately constant on the time scale of the adjustment,

$$(T_t(t) - T_a) = (T_t(0) - T_a) \exp(-t/\tau).$$

or

$$\ln[(T_t(t) - T_a) / (T_t(0) - T_a)] = -t/\tau.$$

Similar values were obtained by determining when 63.2% of the temperature change had been achieved (the standard definition of the time constant) but we considered the line slope method to be more reliable. Results are presented in Table 2 below and show a steady decrease with increasing wind speed. A simulation of the thermocouple wires using an Industrial Thermics package clearly shows that at these wind speeds the centres of the thermocouples are measuring the gas temperature, and are not significantly affected by conducted heat from the frame.

One concern with these initial results is that the actual temperature difference developed between the two flows, as measured with the thermocouples was dependent on the wind speed and had reduced to less than 1 K at a wind speed of 4.5 m/s (See Table 3). Also from Table 3 we note that the RTD temperatures, which are in the same flow, but are not co-located with the TCs, showed different temperatures and temperature differences from the thermocouples. Further investigation of the temperature field within the test section is discussed in the modelling section later in the paper. We have omitted data on the RTD temperatures at 6.8 ms⁻¹ since we suspect an error in recording these.

4.4 WIND TUNNEL RESULTS – TIME CONSTANTS AND TEMPERATURE INCREASES FROM SOLAR RADIATION IMPACTS

In our first attempt at the irradiation tests, the Phoenix thermocouple S/N 221 was used. However we found that the thermocouple unit did not have the anticipated response to the irradiance. After some initial incomprehension we searched for the thermocouple junction using a pen lamp and discovered that it was not in the centre, but at the point where the wire is

attached to the frame. This was reported to MDA and they immediately implemented additional QA/QC procedures and provided new thermocouples with their junctions in the center of the C frame.

Figure 8a shows how the temperature measured by the MDA thermocouple (S/N 207) and the reference temperature measured by the CSIL thermocouple react when the radiation is turned on and off for 20 minute intervals. The MDA thermocouple has a rapid initial response to the radiation followed by a slower adjustment - especially noticeable in the cooling phase. There is a general warming of the whole system, by about 5 degrees in 40 minutes. This appears to be at an approximately constant rate, as indicated by the CSIL thermocouple which is in the dark. Note the different locations of the two TCs in the tunnel which accounts for the approximately 1.6 degree difference between them in the absence of any illumination. As in the flow switching this is associated with diffusion of heat in the laminar flow. Our assumption is that the rapid response (in about 1 s) is the direct heating/cooling of the junction once the illumination commences/ceases while the slower response is linked to the heating/cooling of a longer section of the wire (beyond the test section) and possibly the frame which is being warmed by conduction from the heated junction.

In these tests we are primarily interested in the temperature difference (ΔT) caused by the illumination on long time scales, but Figure 8b shows the fast time evolution of the temperature difference caused by the illumination at different temperatures and wind speeds. The apparent noise is due to a simple lack of resolution in the a/d conversion of our data logger. The delta temperature (ΔT) is calculated as the difference between the final temperature and the initial temperature. The initial temperature is taken as the average temperature during two seconds before the illumination point. It takes about two seconds for the temperature to rise, and the final temperature is the average temperature of two seconds after that rise. We can use these tests to determine a time constant. Table 4 shows the time constant results of the Phoenix thermocouple S/N 207 response to irradiance, as tested on Mar 2, 2006. The reference temperature is measured by York thermocouple. Note that at zero wind speed the time constant for the rapid response phase is about 0.77 sec, while at a higher wind speed (10.8 ms^{-1}) the value is 0.45 sec, in reasonable accord with the values reported in Table 2 from the flow switching tests. In later tests we kept the wind speed approximately constant, and investigated the relationship between the time constant and temperature. Table 5 shows time constant results measured on Mar 7, 2006. Again these are consistent with flow switching results from Table 2, noting the lower wind speed. The time constant appears to increase slightly at low temperatures but note that we have smaller ΔT values at cold temperatures.

Turning to the impacts of simulated solar radiation on the temperatures reported by the thermocouples, we note that the ΔT values in Tables 4 and 5 provide this information. As described in the Solar Radiation and Test Procedures section above, these are intended to represent a maximum likely exposure to solar radiation at mid-sol at the Phoenix site on Mars with relatively low atmospheric attenuation of the solar beam. The irradiance normal to the beam was measured as 473 Wm^{-2} , but there do appear to be problems with optical fibre transmission at very cold temperatures ($< -40\text{C}$). These are apparent in Table 5. The extreme ΔT case is at zero wind speed (Test 2 in Table 4) where the increase is 1.08 C. Once Martian air is flowing past the thermocouple junction and helping to carry away heat the ΔT -

T values decrease to about 0.54 C at a wind speed of 1.8 ms^{-1} . Results for $T > -40\text{C}$ are plotted in Fig 12.

4.5 DUST IMPACTS

As the Phoenix mission proceeds it is possible that there will be a dust deposit on the thermocouple wires and that this could increase the percentage of solar radiation absorbed by them. In an attempt to simulate this, we set up two tests. Two thermocouples were mounted parallel on the same frame and separated about 0.5mm. Dust was sprayed over one of the thermocouples. We used Mars simulant HWMK101 fine dust and magnetic dust (SALTEN SKOV $< 63 \mu\text{m}$, see [Nørnberg et al, 2004](#)) in the two tests. There was more of the magnetic dust stuck on thermocouples. The tests were run over a range of wind speeds. In each test, the first measurement had one wire dusty and the reference wire clean, and the second measurement had both wires clean.

Since every condition such as the position of the thermocouples, wind speeds and pressure were not exact the same during each measurement, some data transformations were needed. Omitting the details and noting that the magnetic dust had the greatest effect we can see from Figure 9 that the effect occurs but, at least in our tests the worst case represents about a 12% increase over the solar radiation effect on a clean wire. We also noted that the dusty wire and the clean wire have virtually simultaneous responses to the radiation, and that dust does not appear to influence the time constant.

4.6 LAMINAR FLOW IN A RECTANGULAR DUCT

In order to investigate the differences in temperature along the test section we considered an idealised situation. First we assumed that, prior to switching the flow the walls of the test section were at the previous temperature (0 after normalisation and scaling). The temperature of the new inflowing air is 1 after normalisation. Ignoring heating of the walls, and ignoring the precise geometry of the test section we consider heat diffusion in a laminar flow in a straight rectangular channel of the correct aspect ratio and with an appropriately calculated velocity profile. Figure 10 illustrates the evolution of the centreline scaled temperature at two centreline flow speeds. The x distance along the tunnel is scaled by the distance from the inlet to the thermocouple location, so that the thermocouple under test is at $x = 1$.

Our wind tunnel tests showed that the temperature differences read by the thermocouples decreased with decreasing wind speed. In tunnel tests we found that at wind speed 2.86 ms^{-1} the temperature difference between cool and warm flows measured by the thermocouple is 0.26C while the difference measured by resistance thermometers which are suspended in the flows before they enter the test section is 3.00C. Only 8.6% of the original temperature remains at the thermocouple location. At a wind speed of 4.95 ms^{-1} the original temperature difference between the two flows is again 3.00C and there is only 0.73C or 24% at the thermocouple.

That result of 3D model shows that 10% and 32% of the entry temperature difference reaches the thermocouples when wind speeds are 2.86m/s and 4.95m/s respectively. This result is consistent with that of our wind tunnel tests and justifies our assumption that heat diffusion can

cause much reduced temperature differences to reach the thermocouple test location, especially as wind speed decreases.

4.7 NUMERICAL FLOW AND HEAT TRANSFER MODELLING

In addition to the idealised flow discussed above we also used a CFD code to more realistically simulate the CSIL Mars wind tunnel. Flow in a section starting from the constriction section in front of the honeycomb and ending before the return curve, was calculated. The 3D simulation solved the flow and thermodynamic equations on an unstructured, locally refined mesh of approximately 3 million nodes using the commercial software ANSYS/CFX 10.0 and calculated on a dedicated Opteron cluster. Second order accuracy was used for spatial and temporal discretizations, including a high resolution blending method for treatment of the advection terms. Results from the full section simulation showed that, although secondary and tertiary flows are present because of the asymmetric form of the constriction, these are an order of magnitude smaller than the main flow. Similarly, flow perturbations caused by the small protrusion of the thermocouple C-frame out of the wall were also found to be an order of magnitude smaller than the streamwise velocity. In the calculated range of test section velocities (2.5 to 25 ms⁻¹), the local Reynolds number based on the thermocouple diameter was at most 7, which along with the laminar flow in the tunnel, clearly does not cause any flow instability.

A small section of the flow in the vicinity of a thermocouple wire (without frame) was used to simulate the wire response time to an ideal step function in the temperature of the incoming flow. The small computational domain was necessary because of the extremely fine mesh required in order to include the solid cylinder body of the wire in the temperature simulation field. The resulting time constant values were generally 30% to 40% below the experimental values given in Table 2, but they matched well with idealized lumped-capacitance estimates. Under these idealized conditions, a time constant of 0.5 s is only reached for flows as low as 1 to 2 ms⁻¹.

The 3D numerical simulations were also employed to investigate the cause for the decreasing temperature differences between hot and cold streams observed in the CSIL wind tunnel with decreasing flow velocity as reported in Table 3. A shorter section of the wind tunnel was employed, but for this simulation the wind tunnel walls were included. Instead of simulating the alternating geometry of the actual wind tunnel, a simulation of two parallel flow sections avoided the need for a costly time dependent geometry and provided sufficient insight to explain the role of the thermally conductive wall material in the homogenization of the temperature fields. To further simplify the problem and to increase the numerical resolution in the region of interest, only the bottom half of the channels was simulated.

The simulation tested two cases, both with CO₂ entering the hot flow section with a temperature 2C above the cold flow section. In one case the inlet velocity was 1 ms⁻¹ and in the other it was 10 ms⁻¹. Figure 11 illustrates the effect of the conductive material (Aluminum) in the exterior and bottom wind tunnel walls in transferring heat between the hot and cold air streams. A low conductivity material used in the middle wall separating the two sections, which corresponded somewhat to the directional flaps of the actual wind tunnel, was clearly

not sufficient to prevent major coupling of the two sides through the wall, especially at low flow rates, when diffusive transport dominates. At higher Reynolds numbers the relative effect of heat conduction through the walls decreases and a higher temperature difference can be maintained between the two flow streams, as the case of 10 ms^{-1} (Fig. 11, bottom) illustrates.

5 CONCLUSIONS

The Mars wind tunnel facility worked well and could be used to determine time constants and potential solar radiation errors as a function of wind speed in a simulated Mars environment. Because of thermal gradients within the test section there were wind-speed dependent differences between temperatures measured with the thermocouples in the centre of the test section and temperatures at the ends, as measured by resistance thermometers. Numerical modelling confirmed that this was due to heat diffusion in the essentially laminar flow through the test section.

Based on results obtained in both flow switching and radiational heating tests, our conclusion is that for wind speeds greater than 5 ms^{-1} the time constant is less than 0.5s, sufficiently short that Phoenix temperature measurements with a time interval of 2s are well matched to the sensor. Low wind speed time constant results were also obtained from the cooling of the thermocouple after input from the solar lamp is shut off (by abruptly closing a window). These results (Tables 4 and 5) allow us to extend the time constant estimates to lower wind speed, and the combined estimates are shown in Figure 12. While there is some temperature dependence, wind speed plays the dominant role in determining the time constant and even at a wind speed of zero there is sufficient heat diffusion to keep the time constant down to 0.77s.

The tests of the impact of solar radiation show that this can cause an apparent increase, or ΔT , in the temperatures reported by a thermocouple exposed to sunlight. These tests were conducted with solar radiation corresponding to Mars with an attenuation of 20% relative to the solar constant. We did not take into account possible enhancement of the solar radiation striking the thermocouples as a result of reflection from the lander surface, but that could possibly lead to additional solar radiation striking the thermocouples. Apart from the anomalous optical fibre effects discussed above the dependence of ΔT on temperature is relatively weak and wind speed has a bigger impact. Figure 12 illustrates the variation with wind speed. Overall we would note that ΔT values of order 1 degree are possible in light winds and high solar radiation. Even with wind speeds of 10 ms^{-1} , errors of order 0.5 degrees are likely at mid sol. However provided that the exposures to sunlight of the thermocouples at all three levels on the mast are similar, then errors in the temperature differences between levels, necessary for the determination of near surface stratification, should remain of order 0.1 degree, and within the specifications expected by the Phoenix Atmospheric Theme Group (ASTG).

6 ACKNOWLEDGEMENTS

The majority of this work has been conducted with support from the Canadian Space Agency through contracts in support of the Phoenix mission. The leader of the overall Phoenix mission is Professor Peter Smith, University of Arizona while Drs Allan Carswell, Diane Michelangeli and James Whiteway have led the MET science team. CSA personnel, Alain Ouellet, Vicky Hipkin and Marcus Dejmek as well as Nilton Renno from University of Michigan have also assisted the science team. Many individuals have worked on the instrumentation and its calibration but in particular we should acknowledge the help of Olajide Akinlade at University of Alberta, Andrew Kerr and Mike Daly at MDA and Stephane Lapensee, Claude Brunet and Isabelle Tremblay at CSA. Jim Tillman from University of Washington provided sage advice as well as expert knowledge of the Viking and Pathfinder instrumentation while Colin Wilson of Oxford University willingly shared his expertise on wind tunnel design.

The principal investigator for MET for much of this time that this project was underway was Professor Diane Michelangeli who sadly passed away in August 2007. Her strong support and enthusiasm for the mission were much appreciated.

7 REFERENCES

- Chamberlain, T. E., H. L. Cole, R. G. Dutton, G. C. Greene and J. E. Tillman, 1976, Atmospheric measurements on Mars: the Viking Meteorology Experiment, *Bul. Amer. Met. Soc.*, 57, 1094-1104.
- H. P. Gunnlaugsson, H.P, Holstein-Rathlou, C., Merrison, J.P., Knak Jensen, S., Lange, C.F., Larsen, S.E., Madsen, M.B., Nørnberg, P., Bechtold, H., Hald, E., Iversen, J.J., Lange, P., Lykkegaard, F., Rander, F., Renno, N., Taylor, P.A., Smith, P., 2008, The Telltale Wind indicator for the Mars Phoenix Lander, *JGR(Planets)* in press.
- Larsen, S.E., Jørgensen, H.E., L. Landberg, L., and Tillman, J.E., 2002, Aspects of the atmospheric surface layers on Mars and Earth, *Boundary-Layer Meteorology*,
- Nørnberg, P., Gunnlaugsson, H.P., Kinch, K., Merrison, J. 2004: Salten Skov I: A Martian dust analogue. Geophysical Research Abstracts, 6, 03168.
- Schofield, J.T., Barnes, J.R., Crisp, D., Haberle, R.M., Larsen, S., Magalhães, J. A., Murphy, J.R., Seiff, A. and Wilson, G., 1997, The Mars Pathfinder Atmospheric Structure Investigation/Meteorology (ASI/MET) Experiment, *Science* 278, 1752-1758.
- Seiff, A., Tillman, J.E., Murphy, J.R., Schofield, J.T., Crisp, D., Barnes, J.R., LaBaw, C., Mahoney, C., Mihalov, J.D., Wilson, G.R. and Haberle, R., 1997, The atmosphere structure and meteorology instrument on the Mars Pathfinder lander, *J. Geophys. Res.*, 102(E2), 4045–4056

Taylor, P.A., Daly, M., Dickinson, C., Gunnlaugsson, H.P., Harri, A-M. and Lange, C.F., 2008, Temperature, Pressure and Wind instrumentation on Phoenix MET, *JGR(Planets)* in press.

Tillman, J. E., Landberg, L., and Larsen, S. E.: 1994, 'The Boundary Layer of Mars: Fluxes, Stability, Turbulence Spectra and Growth of the Mixed Layer', *J. Atmos. Sci.* **51**, 1709–1727.

Zent, A.P., Hecht, M.H, Cobos, D., Cardell, G, Foote, M.C., Woods, S.E. and Mehta, M., 2008, The Thermal Electrical Conductivity Probe (TECP) for Phoenix, , *JGR(Planets)* in press.

APPENDIX A. LIST OF TABLES

	Oxford LDWT	Aarhus Mars Simulation Wind Tunnel	CSIL Mars Wind Tunnel
Wind Speeds	0.5 - 30 m/s	0 – 20 m/s	0 – 30 m/s
Wind Speed Measurement	Orifice plates, measuring the flow rate into the chamber	Laser Doppler anemometer (dust particles)	Pitot Tube
Pressure Range	5 - 10 mbar	5 – 10 mbar	5 – 10 mbar
Temperature Range	currently ambient	153 – 300K	200-300K
Size of Test Section	180 mm diameter	1.5 m length, 400 mm diameter	25 mm x 25 mm x 100-150 mm
Gas used	CO ₂ or dry air	CO ₂	CO ₂ , N ₂ or dry air

Table 1. Basic characteristics of Mars Simulation Wind Tunnels.

Wind Speed(m/sec)	Time Constant for Temperature Decreasing(sec)	Time Constant for Temperature Increasing(sec)
4.5	0.504	0.487
6.8	0.465	0.454
16.0	0.347	0.350
19.0	0.318	0.324
24.3	0.291	0.300
27.7	0.282	0.275

Table 2. Time constant responses to wind speed, switched flow results

Wind Speed (m/sec)	Thermocouple Temp Decreasing			Thermocouple Temp Increasing			RTD		
	High Temp (C)	Low Temp (C)	Temp Difference (C)	High Temp (C)	Low Temp (C)	Temp Difference (C)	High Temp (C)	Low Temp (C)	Temp Difference (C)
4.5	-47.87	-48.88	1.01	-47.90	-48.87	0.98	-40.68	-42.18	1.50
6.8	-47.60	-48.86	1.25	-47.63	-48.84	1.21			
16.0	-46.89	-48.72	1.83	-46.86	-48.69	1.83	-40.10	-41.60	1.50
19.0	-46.46	-48.54	2.08	-46.41	-48.49	2.08	-39.80	-41.30	1.50
24.3	-45.71	-48.29	2.58	-45.65	-48.24	2.59	-39.41	-41.22	1.81
27.7	-44.93	-47.97	3.05	-44.91	-47.96	3.05	-38.90	41.20	2.30

Table 3. Temperature differences of thermocouples and RTD at various wind speeds

	Wind Speed (ms ⁻¹)	Reference Temperature (C)	Pressure (hPa)	Delta-T (C)	Time Constant (sec)
TEST2	0.0	-38.0	7.91	1.080	0.77
TEST1	3.1	-42.1	7.99	0.704	0.67
TEST3	1.6	-32.1	8.12	0.923	0.70
TEST4	4.6	-25.3	8.00	0.705	0.52
TEST5	6.3	-19.9	7.96	0.629	0.51
TEST6	10.8	-14.4	7.99	0.539	0.45
TEST7	2.7	-11.7	8.01	0.774	0.58

Table 4. Temperature increases and time constants of thermocouple response to irradiance, variation with wind speed. Tests are in order of occurrence and increasing temperature.

	Wind Speed (ms ⁻¹)	Reference Temperature (C)	Delta - T (C)	Pressure (hPa)	Time Constant (sec)
TEST1	1.72	-59.3	0.15	7.97	0.75
TEST2	1.71	-53.3	0.35	7.96	0.68
TEST3	1.69	-46.5	0.65	7.96	0.68
TEST4	1.63	-40.2	0.88	7.95	0.64
TEST5	1.65	-34.1	0.89	7.95	0.65
TEST7	1.64	-23.2	0.86	7.96	0.64
TEST8	1.66	-17.2	0.86	7.96	0.63

Table 5. Time constants and temperature increases of thermocouple response to irradiance, effect of varying temperature at low wind speed. Note that lower Delta-T at low reference temperatures (<-40 C) are presumed due to optical fibre transmission problems as discussed earlier in the paper.

APPENDIX B. LIST OF FIGURES

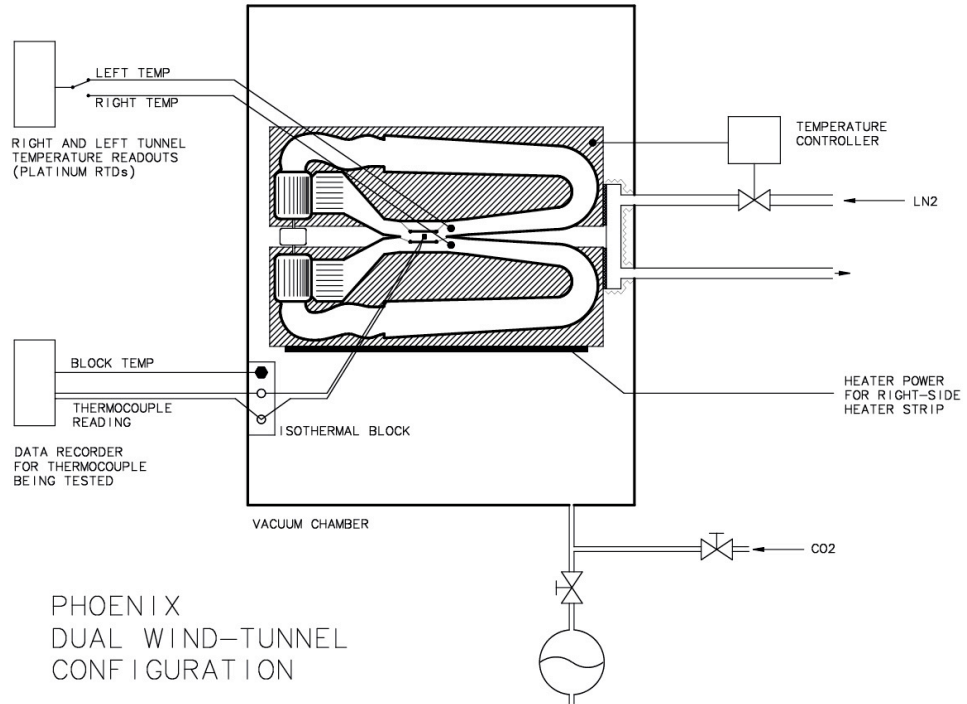


Figure 1: Schematic diagram of the CSIL Mars dual wind tunnel.

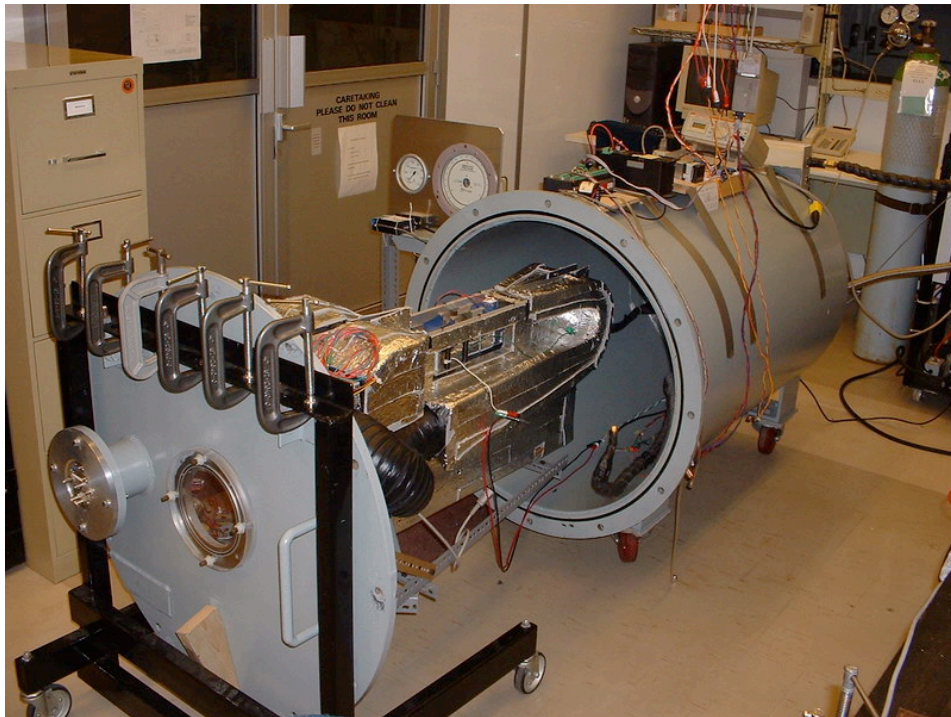


Figure 2 Photograph of the dual wind tunnel and vacuum chamber before being covered with 2nd layer of metallized plastic

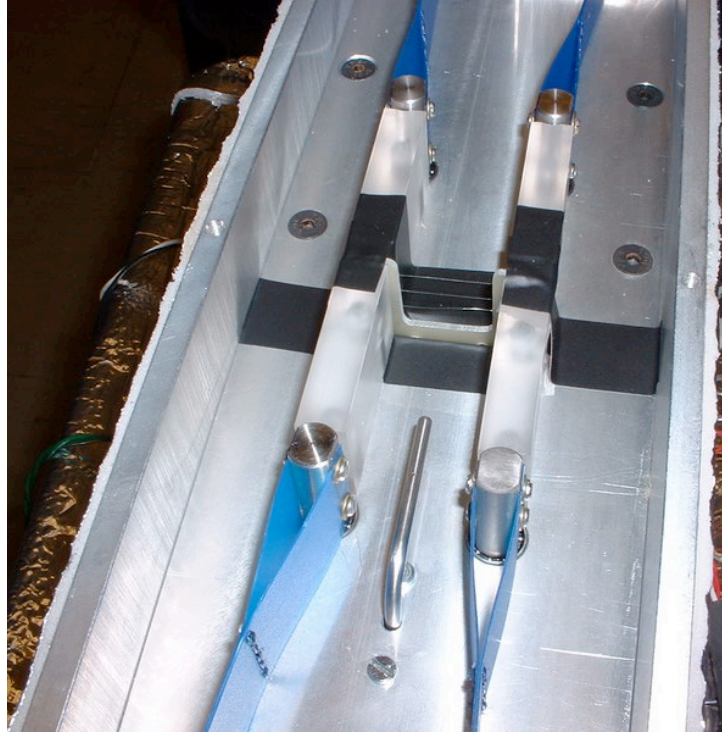


Figure 3. The flow switching test section with a thermocouple frame with three thermocouples installed. Flow is from top to bottom of the picture, towards the Pitot tube. A Perspex lid fits over the top of the section when installed.

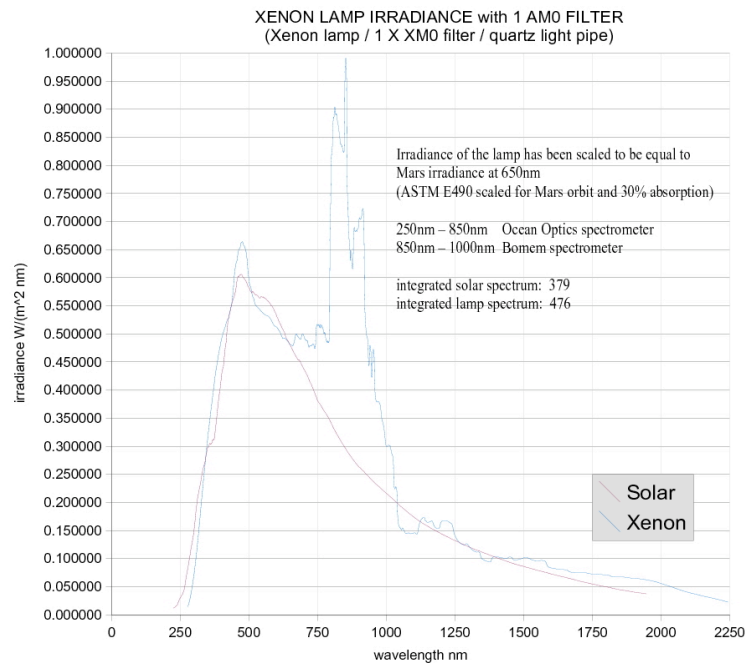


Figure 4. Spectrum of the filtered Xenon lamp output compared to standard solar spectrum.

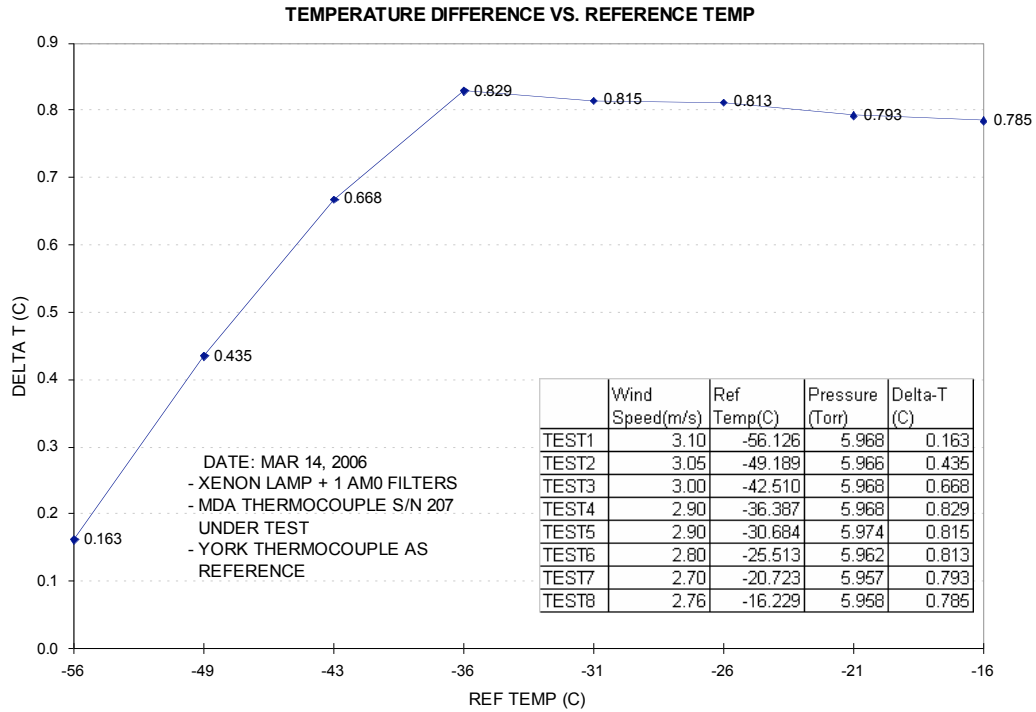


Figure 5. Temperature difference with and without our simulated solar radiation versus reference temperature for wind speeds near 3 ms^{-1} . Note 1 Torr = 1.333 hPa.

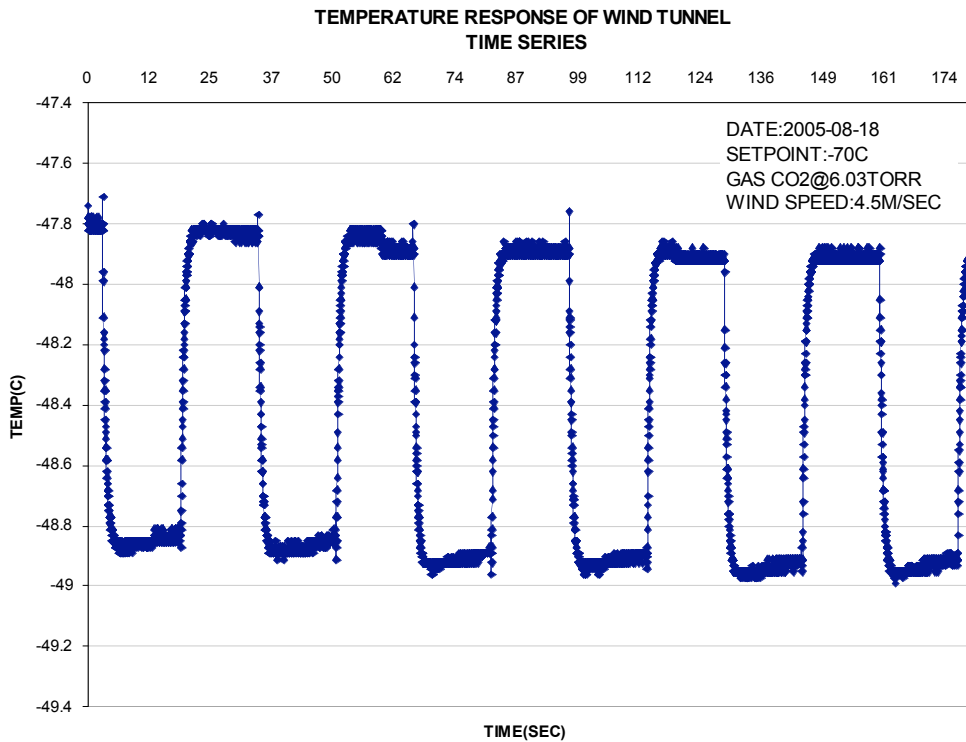


Figure 6. Sample record through 6 temperature cycles with wind speed 4.5 ms^{-1} .

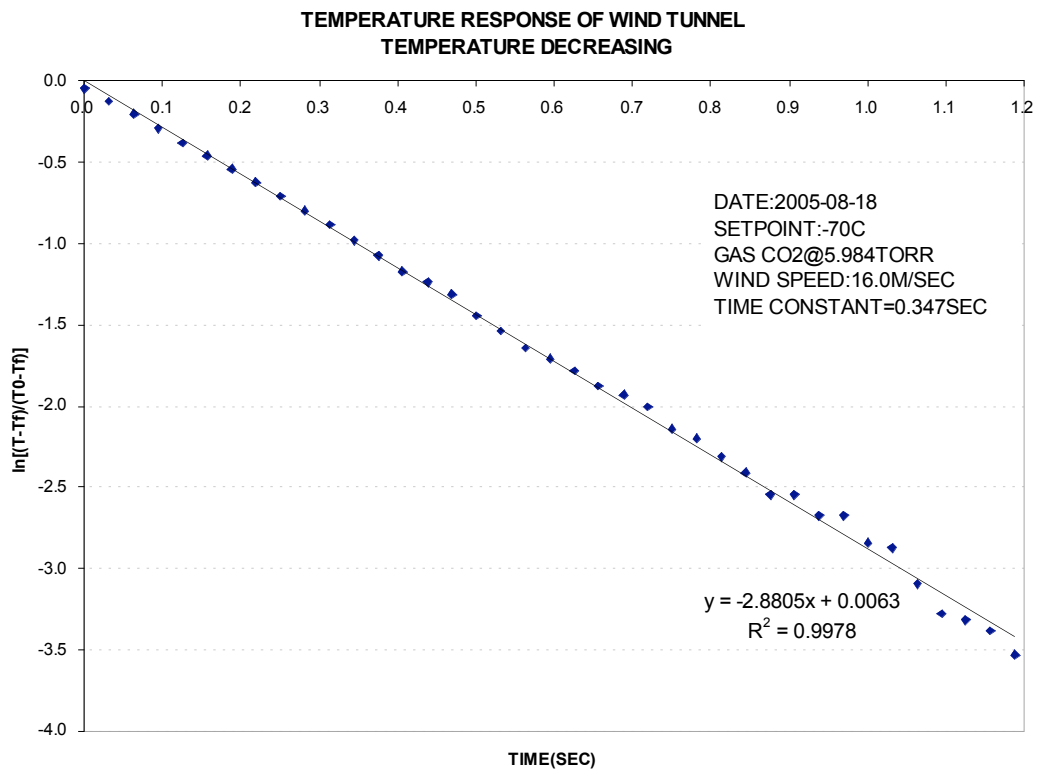
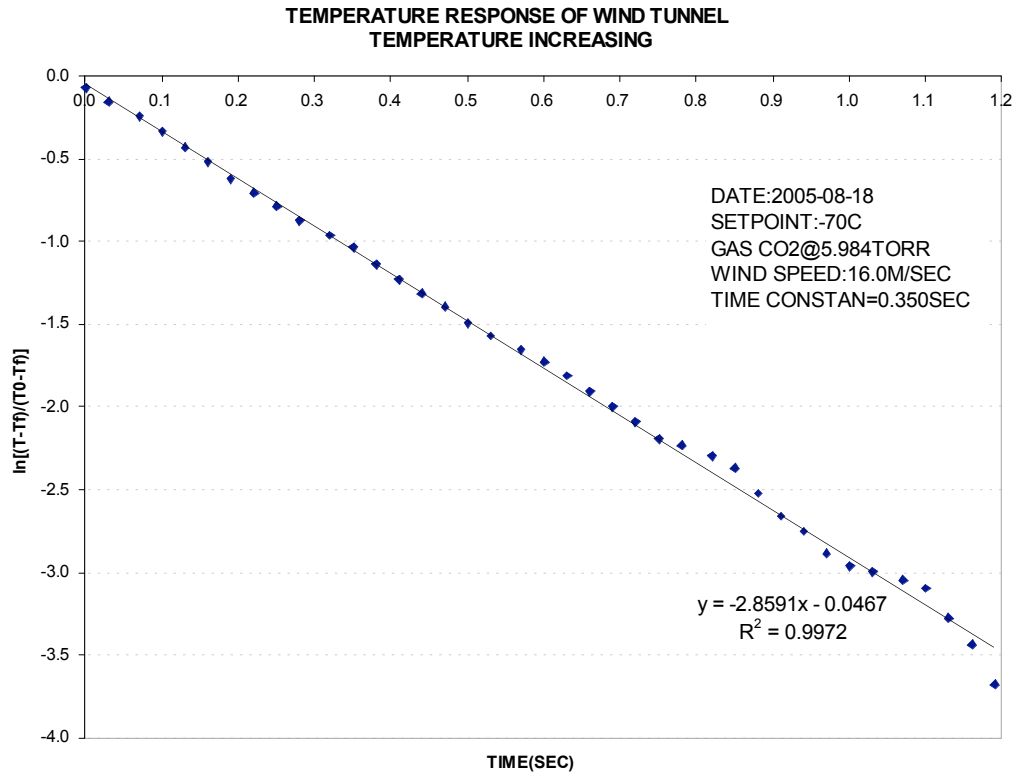


Figure 7. Sample plots used to determine time constants. y axis is $\ln((T-T_f)/(T_0-T_f))$ where T_0 and T_f are the initial and final temperatures

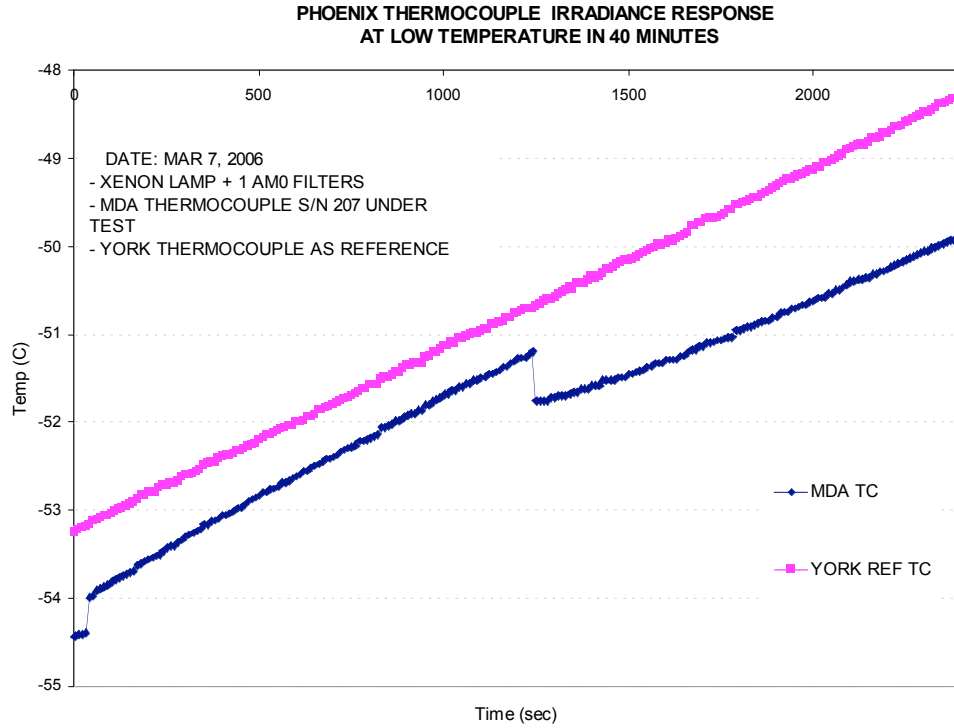


Figure 8a. Thermocouple radiation temperature response curve, Wind speed 1.7 ms^{-1} .

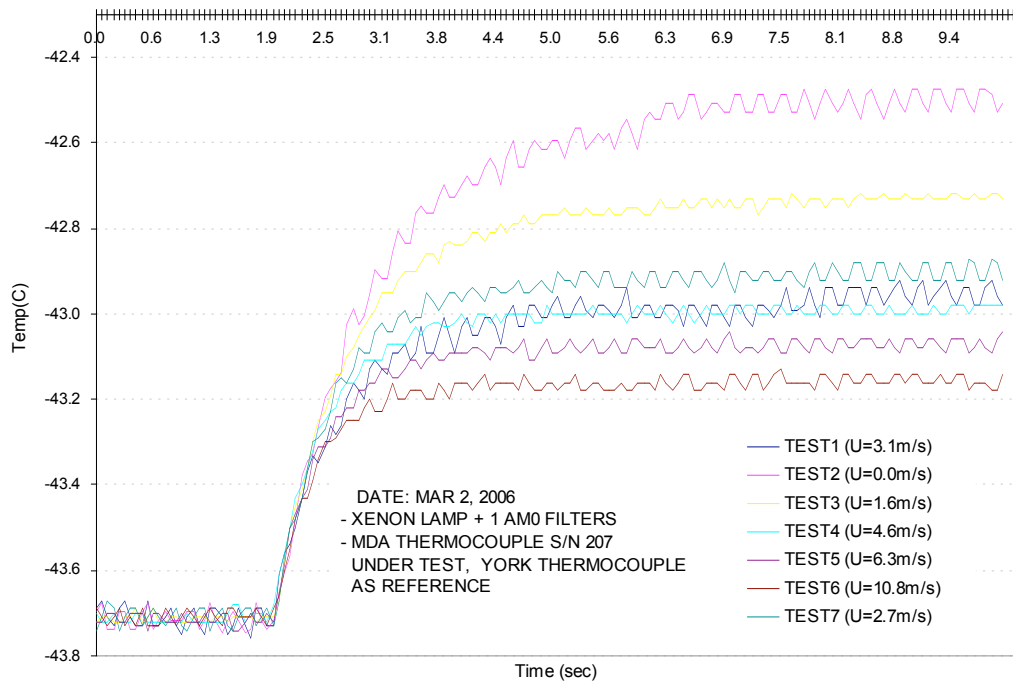


Figure 8b. Temperature short time response to irradiance, wind speeds vary form 0 to 10.8m/s. Temperatures in Tests 1-8 increase from (-42C, -38C, -32C, -25C, -20C, -14C, -12C).

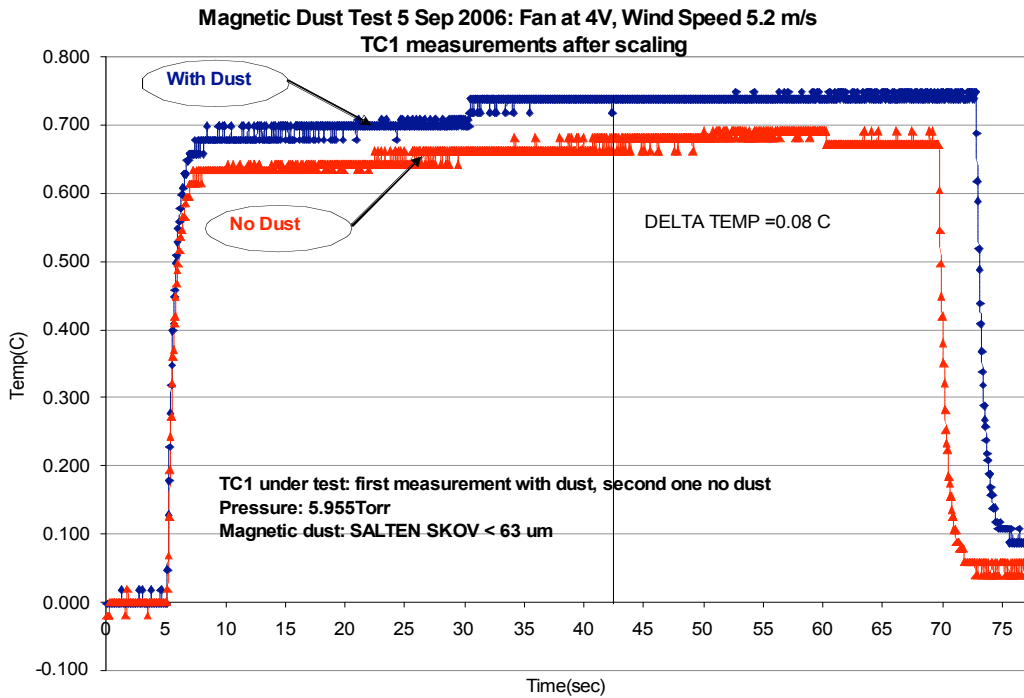


Figure 9: Effect of dust on solar heating, after scaling. Magnetic dust, wind speed 5.2 ms^{-1} .

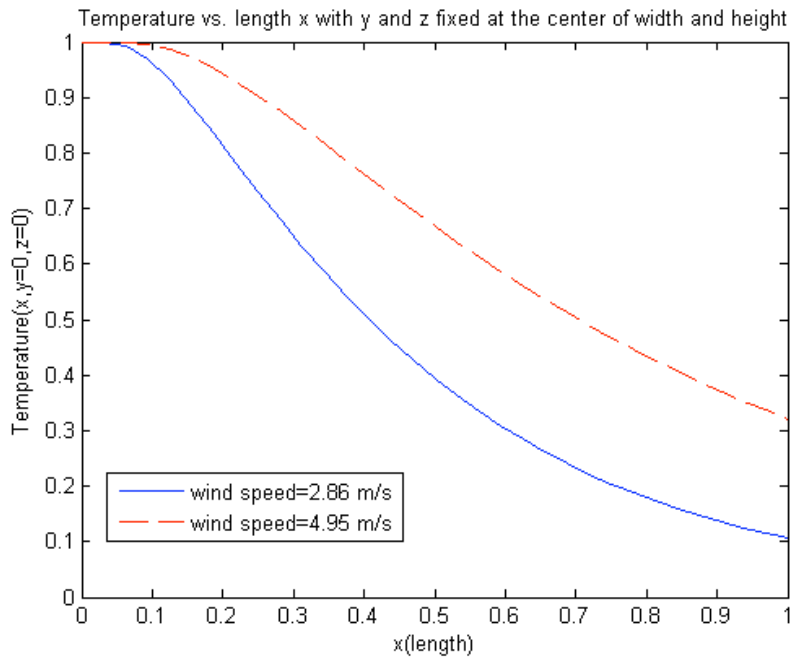


Figure 10. Results from computations with an idealised laminar channel flow for normalised temperature variation at the centre of the channel cross section as it varies with normalised distance along the length of the test section at two wind speeds.

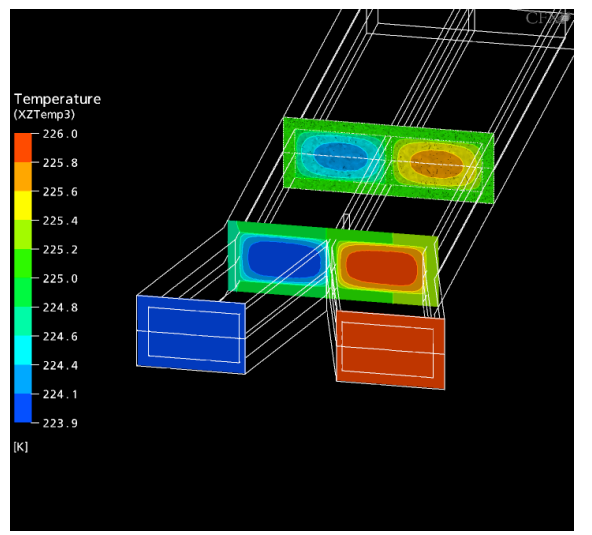
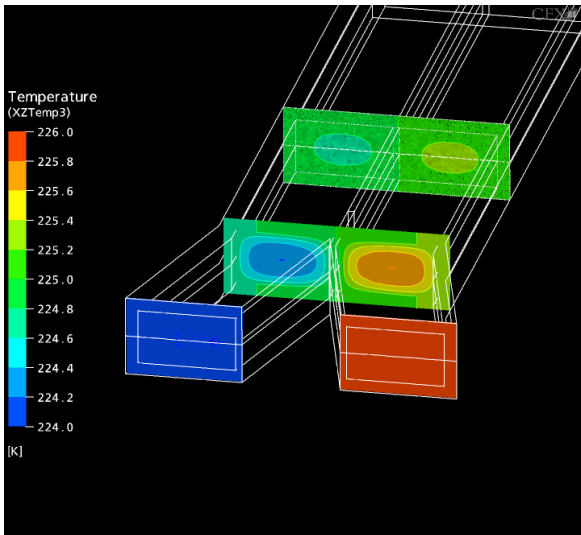
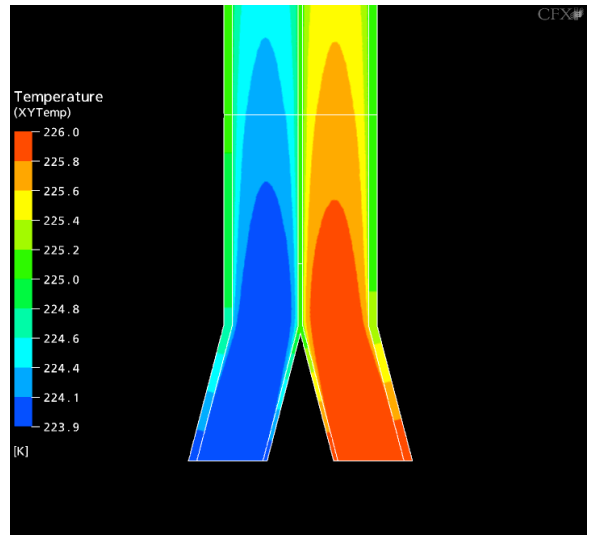
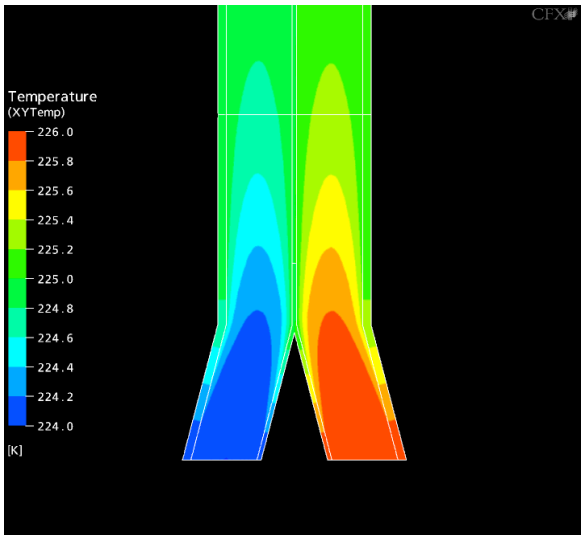


Fig 11 - Steady state temperature contours for $U_{in}=1.0$ m/s (left) and 10 m/s (right) for the XY plane (top) and XZ plane (bottom).

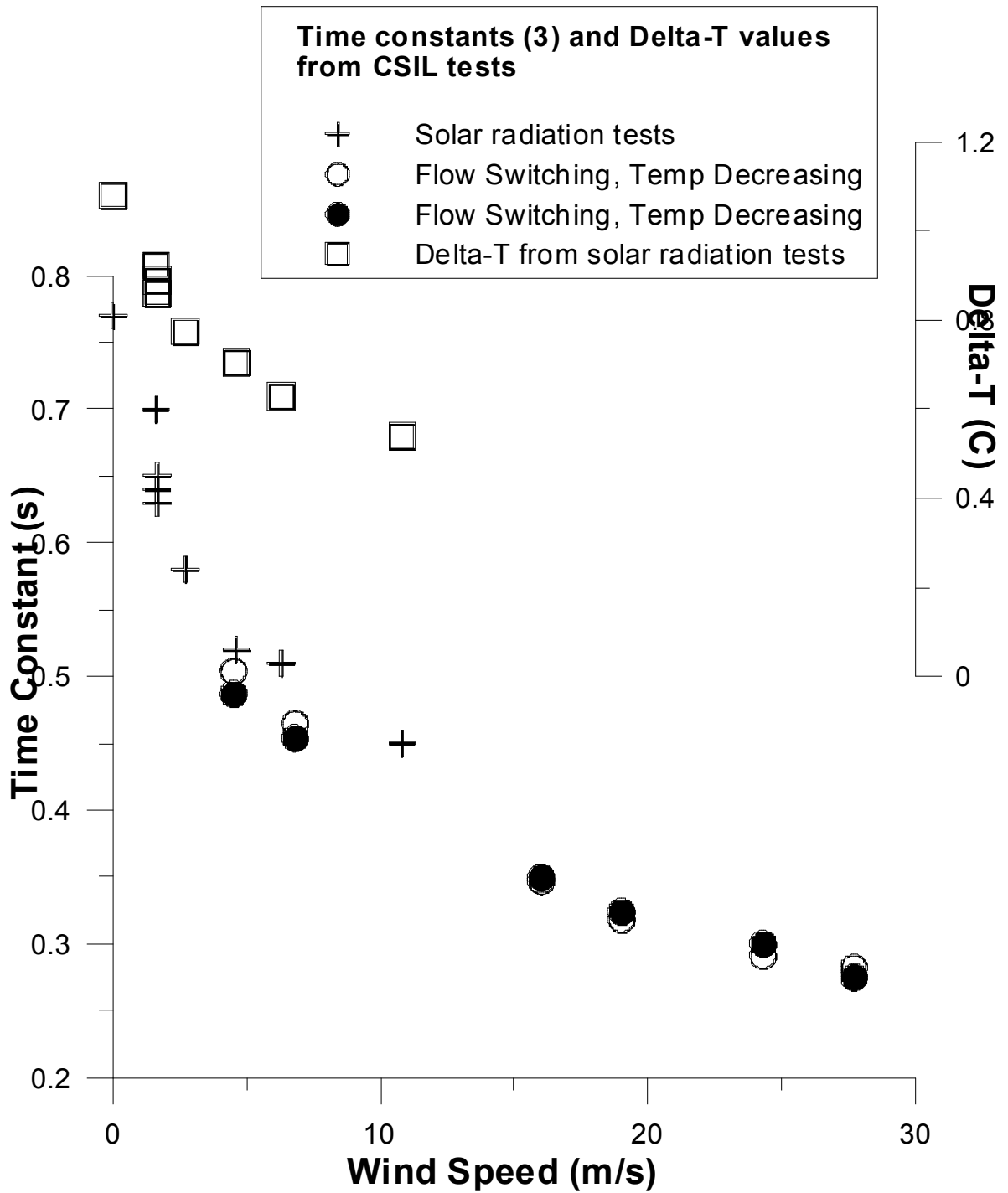


Figure 12. Time constant and Delta-T versus wind speed. Combined data with $T > -40\text{C}$ for several experiments with different thermocouple units